



J. Serb. Chem. Soc. 80 (1) 63–72 (2015)
JSCS–4697

Facile synthesis of water-soluble curcumin nanocrystals

ZORAN M. MARKOVIĆ¹, JOVANA R. PREKODRAVAC¹, DRAGANA D. TOŠIĆ¹,
IVANKA D. HOLCLAJTNER-ANTUNOVIĆ², MOMIR S. MILOSAVLJEVIĆ¹,
MIROSLAV D. DRAMIĆANIN¹ and BILJANA M. TODOROVIĆ-MARKOVIĆ^{1*}

¹Vinča Institute of Nuclear Sciences, University of Belgrade, P. O. Box 522, 11001 Belgrade, Serbia and ²Faculty for Physical Chemistry, University of Belgrade, Studentski trg 14–16, 11000 Belgrade, Serbia

(Received 19 August, revised 12 November, accepted 21 November 2014)

Abstract: In this paper, a facile synthesis of water-soluble curcumin nanocrystals is reported. Solvent exchange method was applied to synthesize curcumin nanocrystals. Different techniques were used to characterize the structural and photophysical properties of the curcumin nanocrystals. It was found that the nanocurcumin prepared by this method had good chemical and physical stability, could be stored in the powder form at room temperature, and was freely dispersible in water. It was established that the size of curcumin nanocrystals varied in the range of 20–500 nm. Fourier transform infrared spectroscopy and UV–Vis analyses showed the presence of tetrahydrofuran inside the curcumin nanocrystals. Furthermore, it was found that the nanocurcumin emitted photoluminescence with a yellow–green color.

Keywords: curcumin nanocrystals; atomic force microscopy; transmission electron microscopy; Raman spectroscopy; photoluminescence spectroscopy.

INTRODUCTION

Curcumin is a natural yellow–orange dye extracted from the rhizomes of the plant *Curcuma longa* L. Commercially available curcumin is a mixture of three curcuminoids, namely, curcumin, demethoxy- and bisdemethoxy-curcumin, the latter two amounting to nearly 30 % in samples labeled “pure”.¹ It shows a remarkable range of pharmacological activity, including antioxidant, anti-inflammatory and anticancer activity.^{2–7} The anticancer potential of curcumin is mediated through the inhibition and modulation of several intracellular signaling pathways, as confirmed in various *in vitro* and *in vivo* cancer studies. Biomedical application of curcumin requires improvement of its bioavailability and its targeting capacity toward cancer tissue. Due to the low bioavailability of curcumin,

* Corresponding author. E-mail: biljatod@vinca.rs
doi: 10.2298/JSC140819117M

numerous approaches were undertaken,^{8,9} *i.e.*, nanoparticle-based drug delivery in which curcumin is encapsulated in liposomes,¹⁰ solid lipid microparticles, such as bovine serum albumin¹¹ and chitosan,¹² or complexed with phospholipids¹³ and cyclodextrin.¹⁴

Various types of nanoparticles, such as polymer nanoparticles, polymeric micelles, liposome/phospholipid, nano-/microemulsions, nanogels, solid lipid nanoparticles, polymer conjugates, self-assemblies, *etc.*, are suitable for the delivery of the active form of curcumin to tumors.¹⁵ Previous studies showed that nanocurcumin has improved anticancer effects as compared to normal curcumin formulations.¹⁶ Bhawana *et al.* demonstrated that the water solubility and antimicrobial activity of curcumin markedly improved by particle size reduction down to the nano range.¹⁷ Recently it was demonstrated that curcumin nanoparticles under aqueous conditions exhibited similar or a much stronger antiproliferative effect on cancer cells compared to normal curcumin in dimethyl sulfoxide (DMSO).¹⁸ Raghavendra *et al.* showed that aqueous-based nanocurcumin (nanoparticles of curcumin) impregnated gelatin cellulose fibers (NCGCFs) has a superior performance over curcumin impregnated gelatin cellulose fibers.¹⁹ The activity of curcumin lies in its ability to scavenge active oxygen- or nitrogen-free radicals.^{6,7,20–22}

Curcumin is practically insoluble in water but soluble in both polar and non-polar organic solvents. It belongs to the group of β -diketones and exhibits tautomerism between enol- and keto-structures (Fig. 1). The relative contributions of the keto and enolic tautomers as well as their *cis* or *trans* form depend on factors such as solvent characteristics, temperature, polarity and substitution on the curcumin.^{23–25} The enol form is characterized by a strong intermolecular hydrogen bond.

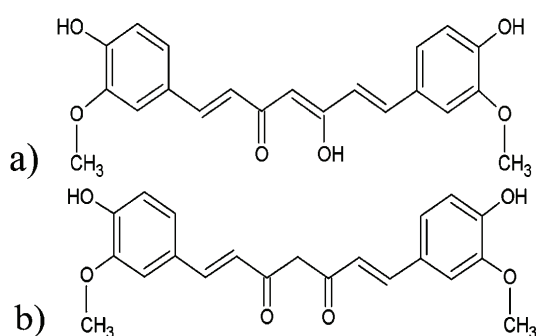


Fig. 1. Structure of the a) enol and b) keto form of curcumin.

In solution, curcumin can form intermolecular H-bonds with the solvent molecules and this strongly influences its physicochemical properties in both the ground and excited states.²⁶ The spectral properties of curcumin show a solvent polarity dependency. Curcumin dissolved in thirteen different solvents (cyclo-

hexane, ethanol, hexane, dichloromethane (DCM), 1,2-dichlorobenzene (DCB), 1,4-dioxane, tetrahydrofuran (THF), methanol, acetonitrile, *n*-butyronitrile (*n*BN), dimethyl sulfoxide (DMSO) and *N,N*-dimethylformamide (DMF)) showed a double-exponential decay function with a short-lived component in the picoseconds time scale.²⁷

Different methods have been applied to synthesize nano-sized curcumin: solvent-based processes, which include emulsification-solvent evaporation,²⁸ emulsification-solvent diffusion, and precipitation methods.^{29,30} Margulis *et al.* demonstrated a method employing turbulent co-mixing of water with a curcumin-loaded emulsion using manually operated confined impingement jet mixers.³¹ Another approach for increasing the rate of dissolution of curcumin is by increasing its surface area. This can be achieved by decreasing the particle size by methods such as milling and grinding.¹⁷

This paper describes facile synthesis of curcumin nanocrystals (nanocurcumin) by means of a solvent exchange method that was previously used regularly for nanoC₆₀ synthesis.³² THF was used to dissolve curcumin before mixing with water. THF is water-miscible organic liquid with low viscosity. This organic solvent transfers their charge to curcumin molecules. This organic solvent is intercalated inside curcumin crystal lattice, thereby improving water solubility. The aim of this paper was to obtain a stable water-soluble nanocurcumin colloid and further investigate its structural and photophysical properties.

EXPERIMENTAL

For the preparation of nanocurcumin colloid, an ethanol extract of commercially obtained curcumin was used. By applying a previously described solvent exchange method,³² the dried ethanol extract was dissolved in fresh THF of HPLC purity (Carlo Erba, Milan, Italy) at a concentration of 1.33 mg mL⁻¹. After purging the mixture with argon to remove any dissolved oxygen, an equal amount of MiliQ water was then added to the THF/curcumin filtrate under continuously stirring. The more volatile THF was subsequently removed from the solution using a rotary evaporator at 45 °C. MiliQ water was added four times more and evaporated to the initial volume. The obtained solution was filtered through a 0.45 μm nylon filter and stored in the dark. After gravimetric estimation, the concentration of the nanocurcumin was adjusted to 0.38 mg mL⁻¹.

The nanocurcumin colloid was characterized by transmission electron microscopy (TEM), atomic force microscopy (AFM), Raman spectroscopy, Fourier transform infrared spectroscopy (FTIR), UV-Vis spectrometry and photoluminescence (PL) spectroscopy.

Transmission electron microscopy imaging was performed on a TEM Philips CM200 microscope operated at 200 kV. Samples were prepared by drop casting a dispersion of nanocurcumin onto a carbon-coated 300 mesh copper grid.

AFM measurements were performed using a Quesant microscope operating in the tapping mode in air at room temperature.³³ Curcumin dissolved in THF and nanocurcumin colloid were deposited on mica substrates by spin coating and imaged after drying. The freshly cleaved mica had a very small roughness (the mean roughness was 0.12 nm) favoring the formation of aggregates which appeared during drying of the thin layer of colloid due to

capillary forces. To reduce aggregation on the substrate, a higher dilution was employed. Standard silicon tips (purchased from NanoAndMore) with a constant force (40 N m^{-1}) were used. The accuracy of the AFM mean diameter determination was improved by deconvolution. The mean diameter of the investigated particles was determined using Gwyddion software.³⁴

The UV–Vis spectra of nanocurcumin suspensions were scanned within the wavelength range of 200–500 nm using an Avantes UV–Vis spectrophotometer. All UV–Vis measurements were performed at 20 °C and automatically corrected for the suspending medium, which was water.

For the FTIR analysis, a nanocurcumin suspension was dried on silicon wafers until thin films were formed. The FTIR spectra were measured at room temperature in the spectral range from 400 to 4000 cm^{-1} on a Nicolet 380 FT-IR, Thermo Electron Corporation spectrometer operating in the ATR mode.

Raman spectra of the nanocurcumin colloid on glass were obtained from a DXR Raman microscope (Thermo Scientific) using 532 nm excitation line from a diode pumped, solid state laser. The laser power was 5 mW. 50× Objectives were used to focus the excitation laser light on the right spot of the investigated samples. The spot size of laser beam was 0.7 μm . The spectral resolution was 0.5 cm^{-1} . The acquisition time was always 100 s (10×10 s).

The photoluminescence spectra of nanocurcumin deposited on SiO_2/Si were recorded at room temperature on a Fluorolog-3 Model FL3-221 spectrofluorometer system (HORIBA Jobin–Yvon). The emission spectra were measured utilizing a 450 W xenon lamp as the excitation source.

RESULTS AND DISCUSSION

Surface morphology of curcumin nanocrystals

Transmission electron microscopy and atomic force microscopy were used to visualize the structure and morphology of the curcumin nanocrystals. The shape and size of the curcumin nanocrystals were determined by AFM. A top view AFM image of curcumin nanoparticles dispersed in THF is presented in Fig. 2a, while AFM image of curcumin nanocrystals dispersed in water and corresponding histogram of nanocurcumin diameters are presented in Fig. 2b. As can be seen from Fig. 2a, the curcumin nanoparticles dissolved in THF had a bagel shape, while the curcumin nanocrystals were spherical. Based on surface analysis the average size of the curcumin nanocrystals was 250 nm. It was also established that about 25 % of the nanocurcumin crystals had a diameter smaller than 100 nm, while 41 % of the nanocurcumin particles had a diameter smaller than 150 nm (Fig. 2d).

TEM micrograph and electron diffraction pattern of nanocurcumin are presented in Fig. 2c. Average size of nanocurcumin based on calculations on large-scale TEM micrographs is about 200 nm. From an electron diffraction image (inset in Fig. 2c), it could be concluded that the nanocurcumin had a crystal structure.

The solubility process is the first step during interactions between polycrystalline curcumin powder and an organic solvent. Curcumin polycrystals obtain charge

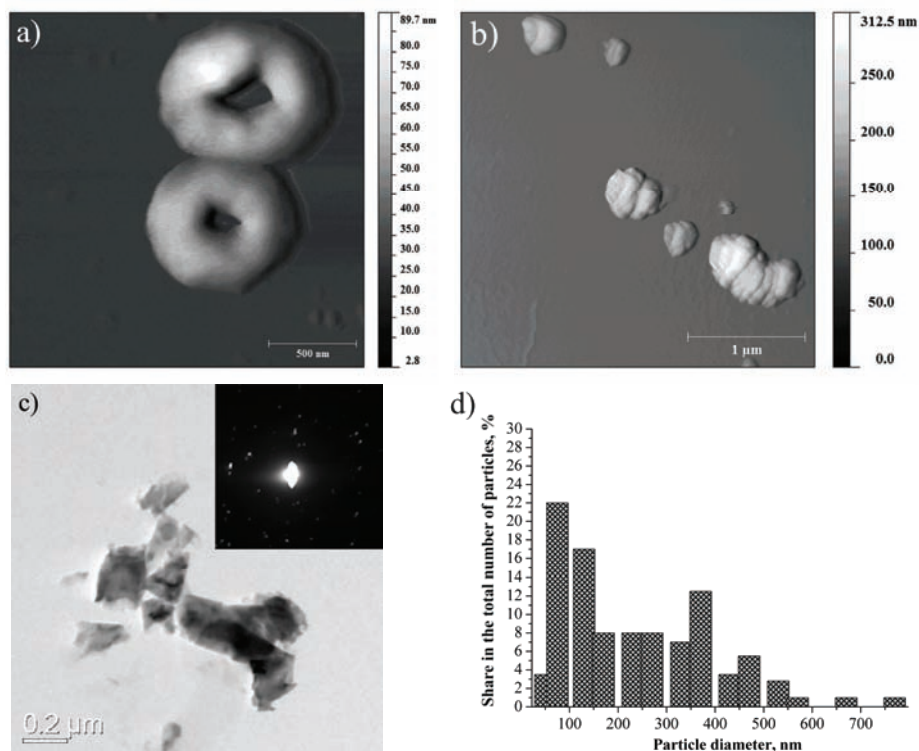


Fig. 2. a) Top-view AFM images of curcumin dissolved in THF and b) water soluble curcumin nanocrystals and the corresponding surface profile; c) bright field TEM micrograph and corresponding electron diffraction pattern of the water-soluble curcumin nanocrystals and d) particle size distribution.

from several thousand THF molecules depending on the size of polycrystal. Tetrahydrofuran is positioned along boundaries of the monocrystals and around the curcumin particles. The nanocurcumin colloid was stabilized electrostatically which was confirmed by its precipitation in 1 wt. % solution. Other authors synthesized curcumin nanoparticles with a narrower particle distribution (2–40 nm)¹⁷ but they used a solvent whose LD_{50} value was lower than that for THF (the amount of a toxic agent sufficient to kill 50 % of a population of animals, usually within a certain time; the LD_{50} value for dichloromethane is 1.6 g kg^{-1} compared to 2–3 g kg^{-1} for THF).³⁵ Average diameter of nanocurcumin produced by solvent exchange method was larger than that produced by the milling and grinding technique due to particle aggregation. In previous investigations concerning nanoC₆₀, it was shown that THF itself is not toxic as it was completely unable to generate reactive oxygen species (ROS) and did not affect cell viability even at the concentrations >100-fold higher³⁶ than its estimated residual presence (10 %) in the nanoC₆₀.³⁷ The solubility of nanocurcumin can be improved significantly

by using polymers such as poly(vinyl pyrrolidone) (PVP), poly(ethylene glycol) (PEG) but the disadvantage of this method is that it requires the addition of considerable amounts of surfactants to prevent coalescence during particle formation.³⁸

FTIR spectra of curcumin nanocrystals

The composition of the prepared nanocurcumin colloid was investigated by FTIR spectroscopy – Fig. 3a. A detailed study on the vibrational spectra of curcumin was reported earlier by Kolev *et al.*³⁹ The FTIR spectrum of curcumin shows characteristic absorption bands at 2852 and 2922 cm^{-1} that represent sp^3 –C–H stretching while the band at 3011 cm^{-1} is due to sp^2 –C–H stretching vibrations. Broad band at 2540 cm^{-1} is due to –O–H stretching vibrations while the broad band between 1980 and 2020 cm^{-1} could be assigned to –C=C–

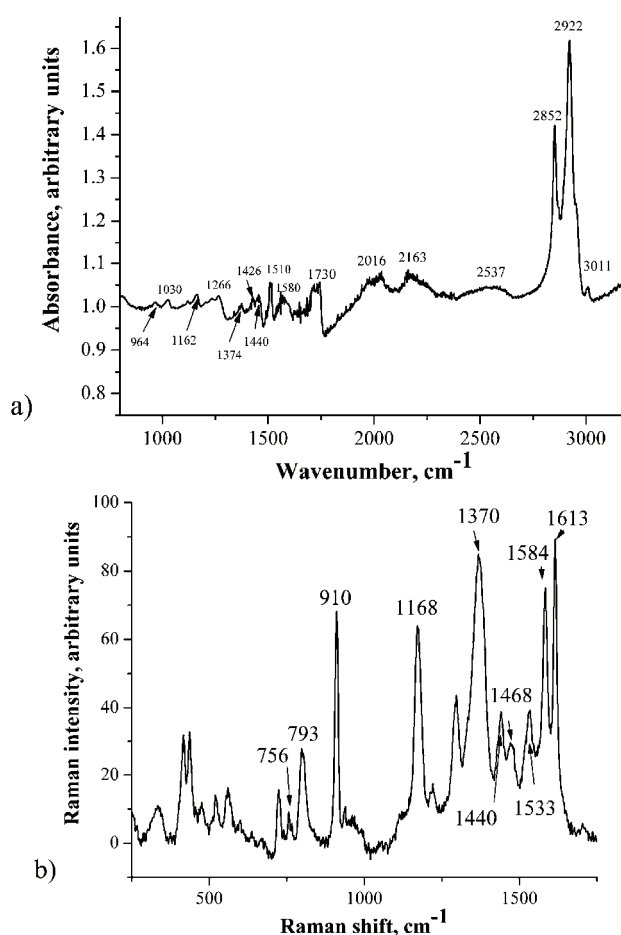


Fig. 3. a) FTIR and b) Raman spectra of nanocurcumin.

asymmetric stretch. The broad band between 1680 and 1730 cm^{-1} corresponds to the -C=O asymmetric mode. The band between 1520 and 1610 cm^{-1} could be assigned to -C=C- in ring while the broad band between 1400 and 1440 corresponds to -CH_3 deformations and the bands at 1030, 1270 and 1160 cm^{-1} stem from -C-O- stretching vibrations. The band at 964 cm^{-1} originates from -C-H bending vibrations.

FTIR analysis of the nanocurcumin colloid revealed two absorption bands at about 2852 and 2922 cm^{-1} , which reflect the presence of strained C-H covalent bonds. The shape and position of the two bands matches perfectly the strongest bands of a tetrahydrofuran liquid film according to the IR spectrum presented in the Spectral Database for Organic Compounds.⁴⁰ Since these two bands do not overlap with typical IR bands of nanocurcumin positioned in the range from 500 to 1800 cm^{-1} , tetrahydrofuran molecules are inserted into interstitial positions of curcumin nanocrystals.

Raman spectra of curcumin nanocrystals

Raman spectroscopy was used in earlier studies for the characterization of curcumin.³⁹ The Raman spectrum of nanocurcumin is shown in Fig. 3b. The peaks at 756 and 793 cm^{-1} seen in Fig. 3b stem from out-of-plane C-C-H bending vibrations while the peak at 910 cm^{-1} originates from in-plane C-C-H bending vibrations. The peaks at 1168, 1440 and 1468 cm^{-1} could be assigned to in-plane -CH_3 bending vibrations while the peak at 1370 cm^{-1} originates from in-plane C-O-H bending vibrations. The peak at 1533 cm^{-1} stem from -C=O stretching vibrations and the peak at 1584 originates from -C-C- stretching vibrations. The peak at 1613 cm^{-1} stems from -C=O stretching vibrations.

Absorption spectra of curcumin nanocrystals

The visible and ultraviolet spectra of organic compounds (such as curcumin) represent transitions between electronic energy levels. These transitions are generally between a bonding or lone-pair orbital and an unfilled non-bonding or anti-bonding orbital. The absorption bandwidth could indicate the degree of agglomeration.⁴¹ The UV-Vis spectra of curcumin dissolved in ethanol and THF as well as of nanocurcumin are presented in Fig. 4a and b, respectively. The UV-Vis spectra of curcumin dissolved in ethanol and THF (Fig. 4a) overlap while the UV-Vis spectra of curcumin dissolved in THF and nanocurcumin differ (Fig. 4b). As can be seen, there is one peak at 427 nm that could be assigned to low-energy $\pi-\pi^*$ excitation of the chromophore (this peak is typical for curcumin dissolved in organic solvent such as tetrahydrofuran – curve 1) and one shoulder at 279 nm. As for nanocurcumin, there is a very broad absorption band at 410 nm and a shoulder (weak absorption band) at 283 nm – curve 2. A blue shift to 410 nm and broadening of the absorption peak at 427 nm due to effect of water were

registered. The intensity of the absorption peak at 410 nm was also significantly reduced. The evolution of absorption peak at 410 nm for the π - π^* transitions of curcumin in water as well as the decreasing intensity indicate a change in the tautomeric form of the keto-enol-enolate group in curcumin. The broadening of absorption band at 410 nm was caused by aggregation of the nanocrystals.

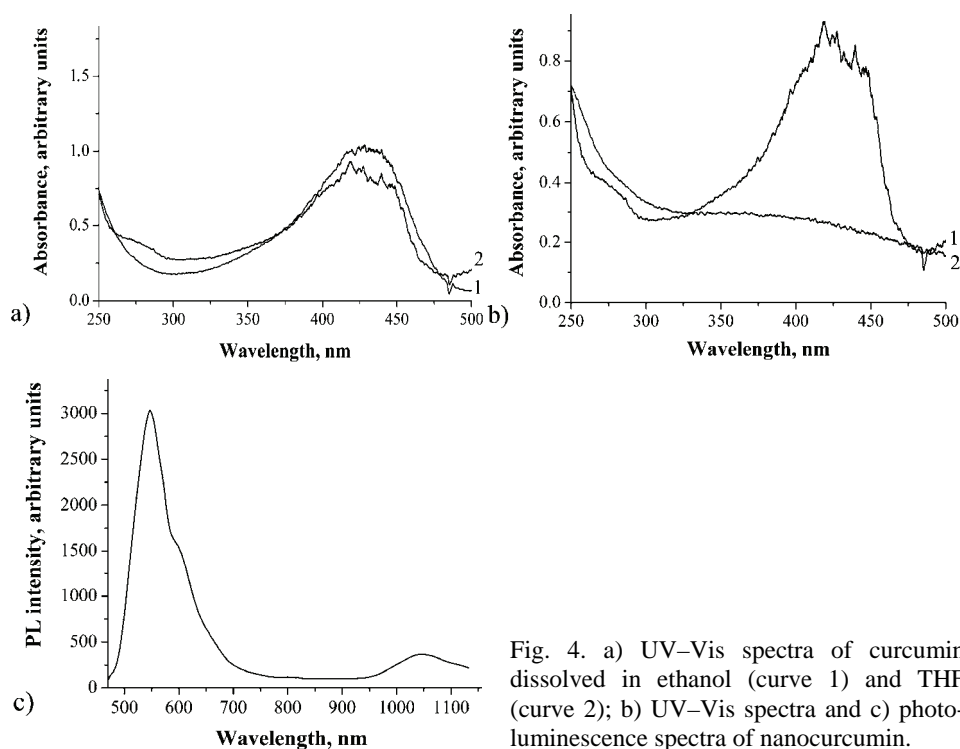


Fig. 4. a) UV-Vis spectra of curcumin dissolved in ethanol (curve 1) and THF (curve 2); b) UV-Vis spectra and c) photoluminescence spectra of nanocurcumin.

Photoluminescence spectra of curcumin nanocrystals

A photoluminescence spectrum of nanocurcumin is presented in Fig. 4c. Under excitation of 405 nm, there are two PL peaks at 547 and 595 nm, and their intensities decreased rapidly. One of the possible explanations for the multiple peaks could be variation in the size of the crystallites, and the emission would have come from a statistical average of the crystallites. The solvent polarity affects (the effect of THF) intramolecular charge transfer, which influences the fluorescence emission. Polar solvents also shift the emission to longer wavelength due to the stabilization of the excited states.⁴²

CONCLUSIONS

In this paper, a facile synthesis of water-soluble curcumin nanocrystals was presented. It was established that the most important features of synthesized

colloid were: the average size of the photoluminescent curcumin nanocrystals was around 250 nm and their long-term stability. Due to very low toxicity of tetrahydrofuran, nanocurcumin colloids could be applied in nanomedicine.

Acknowledgement. This research was supported by the Ministry of Education, Science and Technological Development of Republic of Serbia (Project No. 172003).

ИЗВОД

СИНТЕЗА ВОДОРАСТВОРНИХ НАНОКРИСТАЛА КУРКУМИНА

ЗОРАН М. МАРКОВИЋ¹, ЈОВАНА Р. ПРЕКОДРАВАЦ¹, ДРАГАНА Д. ТОШИЋ¹, ИВАНКА Д. ХОЛЦЛАЈТНЕР-АНТУНОВИЋ², МОМИР С. МИЛОСАВЉЕВИЋ¹, МИРОСЛАВ Д. ДРАМИЋАНИН¹
и БИЉАНА М. ТОДОРОВИЋ-МАРКОВИЋ¹

¹Институт за нуклеарне науке „Винча“, Универзитет у Београду, Мике Аласа 12–14, 11001 Београд и
²Факултет за физичку хемију, Универзитет у Београду, Свуденски Три 14–16, 11000 Београд

У раду је приказан нови начин синтезе нанокристала куркумина применом методе измене растварача. За испитивање структурних и фотофизичких особина нанокристала куркумина коришћене су различите технике карактеризације. Утврђено је да колоид нанокуркумина припремљен овим поступком има добру физичку и хемијску стабилност и да се лако раствара у води. Применом микроскопије атомске силе утврђено је да је величина нанокристала куркумина била у опсегу од 20–50 nm. Фуријеова инфрацрвена и UV–Vis спектроскопија су показале присуство тетрахидрофурана унутар нанокристала куркумина. Такође је утврђено да нанокуркумин емитује фотолуминесценцију у жуто-зеленој области спектра.

(Примљено 19. августа, ревидирано 12. новембра, прихваћено 21. новембра 2014)

REFERENCES

1. F. Jasim, F. Ali, *Microchem. J.* **38** (1988) 106
2. O. P. Sharma, *Biochem. Pharmacol.* **25** (1976) 1811
3. T. Masuda, Y. Toi, H. Bando, T. Maekawa, Y. Takeda, H. Yamaguchi, *J. Agric. Food Chem.* **50** (2002) 2524
4. K. Mehta, P. Pantazis, T. McQueen, B. Agarval, *Anti-Cancer Drugs* **8** (1987) 471
5. A. N. Nurfini, M. S. Reksoha Diprodjo, H. Timmerman, U. Jenie, D. Sigianto, H. J. van der Goot, *Med. Chem.* **32** (1997) 321
6. N. Sreejayan, M. N. A. Rao, K. I. Priyadarsini, A. T. P. Devasagayam, *Int. J. Pharm.* **151** (1997) 127
7. P. Venkatesan, M. N. Rao, *J. Pharm. Pharmacol.* **52** (2000) 1123
8. P. Anand, A. B. Kunnumakkara, R. A. Newman, B. B. Aggarwal, *Mol. Pharm.* **4** (2007) 807
9. P. Anand, H. B. Nair, B. Sung, A. B. Kunnumakkara, V. R. Yadav, R. R. Tekmal, B. B. Aggarwal, *Biochem. Pharmacol.* **79** (2010) 330
10. D. Wang, M. S. Veena, K. Stevenson, C. Tang, B. Ho, J. D. Suh, V. M. Duarte, K. F. Faull, K. Mehta, E. S. Srivatsan, M. B. Wang, *Clin. Cancer Res.* **14** (2008) 6228
11. V. Gupta, A. Aseh, C. N. Rios, B. B. Aggarwal, A. B. Mathur, *Int. J. Nanomed.* **4** (2009) 115
12. R. K. Das, N. Kasoju, U. Bora, *Nanomedicine* **6** (2010) 153
13. K. Maiti, K. Mukherjee, A. Gantait, B. P. Saha, P. K. Mukherjee, *Int. J. Pharm.* **330** (2007) 155

14. M. M. Yallapu, M. Jaggi, S. C. Chauhan, *Macromol. Biosci.* **10** (2010) 1141
15. I. Muqbil, A. Masood, F. H. Sarkar, R. M. Mohammad, A. S. Azmi, *Cancers* **3** (2011) 428
16. G. Flora, D. Gupta, A. Tiwari, *Crit. Rev. Ther. Drug* **30** (2013) 331
17. R. Bhawana, H. Kumar Basniwal, V. K. Singh Buttar, N. Jain, *J. Agr. Food Chem.* **59** (2011) 2056
18. R. Kumar Basniwala, R. Khoslab, N. Jain, *Nutr. Cancer* **66** (2014) 1015
19. G. Raghavendra, T. Jayaramudu, K. Varaprasad, S. Ramesh, K. Mohana Raju, *RSC Adv.* **4** (2014) 3494
20. M. Onoda, H. Inano, *Nitric Oxide* **4** (2000) 505
21. A. Gorman, V. Hamblett, V. Srinivasan, P. Wood, *Photochem. Photobiol.* **59** (1994) 389
22. K. Priyadarsini, *Free Radic. Biol. Med.* **23** (1997) 838
23. C. F. Chignell, P. Bilski, K. J. Reszka, A. G. Motten, R. H. Sik, T. A. Dahl, *Photochem. Photobiol.* **59** (1994) 295
24. V. Galasso, B. Kovac, A. Modelli, M. F. Ottaviani, F. Pichierri, *J. Phys. Chem., A* **112** (2008) 2331
25. S. M. Khopde, K. I. Priyadarsini, D. K. Palit, T. Mukherjee, *Photochem. Photobiol.* **72** (2000) 625
26. L. Nardo, R. Paderno, A. Andreoni, M. Masson, T. Haukvik, H. H. Tonnesen, *Spectroscopy* **22** (2008) 187
27. D. Patra, C. Barakat, *Spectrochim. Acta, A* **79** (2011) 1034
28. M. K. Modasiya, V. M. Patel, *Int. J. Pharm. Life Sci.* **3** (2012) 1490
29. Y.-M. Tsai, C.-F. Chien, L.-C. Lin, T.-H. Tsai, *Int. J. Pharm.* **416** (2011) 331
30. M. Kakran, N. G. Sahoo, I. L. Tan, L. Li, *J. Nanopart Res.* **14** (2012) 757
31. K. Margulis, S. Magdassi, H. S. Lee, C. W. Macosko, *J. Colloid Interf. Sci.* **434** (2014) 65
32. S. Deguchi, G. A. Rossitza, K. Tsujii, *Langmuir* **17** (2001) 6013
33. B. Todorović-Marković, S. Jovanović, V. Jokanović, Z. Nedić, M. Dramićanin, Z. Marković, *Appl. Surf. Sci.* **255** (2008) 3283
34. Gwyddion, <http://www.gwyddion.net> (accessed on July 20th, 2014)
35. D. E. Moody, *Drug. Chem. Toxicol.* **14** (1991) 319
36. Z. Marković, B. Todorović-Marković, D. Kleut, N. Nikolić, S. Vranješ-Djurić, M. Misirkić, L. Vučićević, K. Janjetović, A. Isaković, L. Harhaji, B. Babić-Stojić, M. Dramićanin, V. Trajković, *Biomaterials* **36** (2007) 5437
37. L. Harhaji, A. Isaković, N. Raičević, Z. Marković, B. Todorović-Marković, N. Nikolić, S. Vranješ-Djurić, I. Marković, V. Trajković, *Eur. J. Pharmacol.* **568** (2007) 89
38. S. D. Kumavat, Y. S. Chaudhari, P. Borole, K. Shenghani, P. Duvvuri, N. Buber, P. Shah, *Int. J. Pharm. Research Sci.* **2** (2013) 693
39. T. M. Kolev, E. A. Velcheva, B. A. Stamboliyska, M. Spitteller, *Int. J. Quantum Chem.* **102** (2005) 1069
40. SDBS Compounds and Spectral Search, http://sdb.sdb.aist.go.jp/sdb/cgi-bin/direct_frame_top.cgi (accessed on July 21th, 2014)
41. J. Lee, J. H. Kim, *Environ. Sci. Technol.* **42** (2008) 1552
42. J. Lakowicz, *Principles of Fluorescence Spectroscopy*, 3rd ed. Springer, New York, 2006.